Taylor & Francis
Taylor & Francis Group

Non-Maxwell slippage induced by surface roughness for microscale gas flow: a molecular dynamics simulation

BING-YANG CAO*

Department of Engineering Mechanics, Tsinghua University, Beijing, 100084, China

Rarefied gas flows in rough microchannels are investigated by non-equilibrium molecular dynamics simulations. The surface roughness is modelled by an array of triangular modules. The Maxwell slip model is found to break down due to the surface roughness for gas flows in microchannels with large surface roughness. Non-Maxwell slippage shows that the slip length is smaller than that predicted by the Maxwell model and is nonlinearly related to the mean free path. For larger surface roughness and smaller Knudsen number, the non-Maxwell effect becomes more pronounced. The boundary conditions, generally including velocity slip, no-slip and negative slip, depend not only on the Knudsen number but also on the surface roughness. Simulation results show that $A/\lambda \approx 1$ is a good criterion to validate the no-slip boundary condition and $A/\lambda > 0.3$ can be a criterion to judge the occurrence of non-Maxwell slippage, where A is the surface roughness size and λ is the mean free path of gas molecules. The permeability enhanced by the surface roughness may be responsible for the roughness-induced non-Maxwell slippage.

1. Introduction

Due to the rapid advancement of micromachining technology over recent decades, it has been feasible to fabricate microscale to nanoscale devices, such as MEMS and NEMS (micro/nano-electromechanical systems) [1, 2]. Understanding the physics of fluid flows at micro and nanoscale is crucial to designing, optimizing, fabricating and utilizing such MEMS and NEMS-based devices [3–5]. A number of reports in the literatures have shown that fluid flows at micro and nanoscale differ greatly from those at macroscale and the Navier–Stokes equations with no-slip boundary condition, as routinely applied for macroscale fluidics, are incapable of modelling the phenomena occurring in micro and nanoscale devices [6, 7]. One of the most significant reasons is that fluids flowing over a solid surface actually do slip and the conventional no-slip boundary condition is merely an approximation at macroscale [8, 9]. For gas flows in microscale devices, four regimes, i.e. continuum, slip, transition and free-molecule flow, are experientially classified according to the Knudsen number, *Kn*, which is defined as the ratio of the molecular mean free path, λ, to the characteristic

length of a flow system, H ($Kn = \lambda/H$). For $0.001 < Kn < 0.1$, gas flows at microscale fall into the slip regime, where a slip boundary condition has to be applied along with the Navier–Stokes equations [6–11]. It was demonstrated that operation of most of the recently developed MEMS-based devices, such as micropumps, microaccelerometers, microvalves, micro-nozzles and flow sensors, should be characterized by fluidic models with a slip boundary condition (see figure 1.10 in [12]). Therefore, knowing the boundary slip of microscale gas flows is highly desirable.

Maxwell first derived an expression to describe the slip boundary condition of gases flowing over a solid from considerations of the kinetic theory of dilute and atomic gases [13]. The Maxwell model shows that the slip length is linearly related to the mean free path by

$$L_s = \frac{2-f}{f}\lambda \tag{1}$$

in which L_s is the slip length, λ is the mean free path of molecules and f is the tangential momentum accommodation coefficient (TMAC), namely the fraction of molecules reflected diffusively from a solid surface. The expression for the slip boundary condition has been widely applied in rarefied gas dynamics and microscale

*Email: caoby@tsinghua.edu.cn

gas flows [10, 12]. However, solid walls analysed in the Maxwell model are essentially assumed to be mathematically smooth, which means that the surface roughness of the walls should be so small as to be neglected when compared with the molecular mean free path. However, this assumption may not be valid for gas flows in microdevices. For example, the mean free path of air at the standard condition is about $0.065\,\mu m$, which is comparable with the surface roughness in silicon-based microdevices [14, 15].

The surface roughness was first demonstrated to affect the boundary conditions of fluid flows by Richardson [16]. He considered a continuum fluid passing a corrugated wall to show that the no-slip boundary condition was just an inevitable consequence of the surface roughness. Volkov's Monte Carlo simulations [17] revealed a decreased slip of gas flows when progressively higher surface roughness was considered. That may also present explanation for Sun *et al.*'s recent results that the surface roughness simulated by a direct simulation Monte Carlo method caused a significant increase in the friction factor of gas flows in microchannels [18]. Unfortunately, the Monte Carlo method has to adopt the Maxwell assumption for gas–solid interactions. Using molecular dynamics (MD) simulations, Mo *et al.* [19] demonstrated that the no-slip boundary condition arose when the molecular mean free path was comparable with the roughness size A. They then introduced the ratio of the mean free path to the roughness size λ/A to judge the no-slip boundary condition for rarefied gas flows in microchannels. Recently, Sugiyama *et al.* [20] and Turner *et al.* [21] measured experimentally the friction of gas flows in microchannels and found that the surface roughness could lead to a larger friction than the predictions of the Maxwell model. Cao *et al.* [22, 23] applied molecular dynamics simulations to study the roughness effect on microscale gas flows. They observed that the surface roughness often caused a less slip and a larger friction compared with those predicted by the Maxwell model. Thus, we question the applicability of the Maxwell model for rarefied gas flows in microchannels.

In this paper non-equilibrium molecular dynamics simulation is applied to investigate rarefied gas flows in submicron channels with surface roughness which is modeled by an array of triangular modules. A non-Maxwell slippage induced by the surface roughness is observed. This non-Maxwell behaviour shows that the slip length is smaller than the prediction of the Maxwell model and is nonlinearly related to the mean free path. A criterion characterized by the ratio of the surface roughness to the mean free path is then put forward to demonstrate the non-Maxwell effect. In section 2, we present simulation details and analysis method.
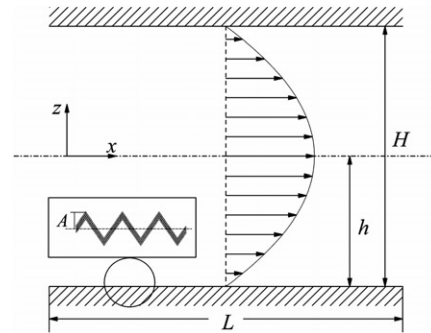
Figure 1. Schematic diagram of the simulation system. The inserted sub-figure is an array of triangular roughness units.

In section 3, simulation results are presented. Finally, in section 4, we conclude.

2. Simulation and analysis methods

2.1. *Simulation details*

Using the method of two-dimensional molecular dynamics simulation, we study the dynamics of N argon molecules enclosed between two parallel platinum walls as shown in figure 1. As the computation efficiency of the two-dimensional molecular dynamics method is much higher than the traditional molecular dynamics [24], the distance between the two plates reaches $H = 0.10\,\mu m$ ($h = H/2$), which is really comparable with the scale of microdevices in engineering situations. In all our simulation cases, the channel size is fixed and the Knudsen number is varied by changing the density of the gas. A Poiseuille flow is induced by subjecting the molecules to an external gravitational field, g_x [25]. $g_x = 3.7 \times 10^{11}\,m/s^2$ is adopted for flows in rough microchannels and $1.85 \times 10^{11}\,m/s^2$ is used for flows in smooth microchannels. The flows are locally fully developed to be laminar with Reynolds numbers (Re) in the range of 5–50. In the x direction, the size of the simulation cell is about $L = 0.1\,\mu m$. A periodic boundary condition is imposed along the x direction.

The surface roughness is modeled by an array of triangular modules with a size of A. We set the centrelines of the roughness geometries to be the boundaries of the microchannels, which agrees with the traditional choice of most researchers [26]. To maintain a realistic gas-solid interaction, we build atomic structure walls based on the Einstein theory that the platinum atoms vibrate around the face-centered-cubic (FCC) [1,1,1] lattice sites with the Einstein

frequency tethered by a harmonic spring with the stiffness of

$$k = \frac{16\pi^4 k_B^2 m^2 \theta}{h^2} \qquad (2)$$

in which k_B is the Boltzmann constant, h is the Planck constant, m is the mass of a wall atom and $\theta = 180\,\mathrm{K}$ is the Einstein temperature of platinum. The stiffness is also examined to follow the Lindemann criterion [27].

Particle interactions with each other are via a Lennard–Jones (LJ) 6–12 potential

$$\phi(r) = 4\varepsilon \left[\left(\frac{\sigma}{r}\right)^{12} - \left(\frac{\sigma}{r}\right)^{6} \right] \qquad (3)$$

where r is the intermolecular distance, ε is the energy of potential well and σ is the molecular diameter. The parameters are respectively $\varepsilon_{\mathrm{Ar-Ar}} = 1.67 \times 10^{-21}$ J, $\sigma_{\mathrm{Ar-Ar}} = 3.405 \times 10^{-10}$ m, $\varepsilon_{\mathrm{Ar-Pt}} = 0.894 \times 10^{-21}$ J and $\sigma_{\mathrm{Ar-Pt}} = 3.085 \times 10^{-10}$ m [28]. The argon-platinum interaction corresponds to a wettability measured by a contact angle of about $35°$ for a flat surface [29, 30]. The molecules move according to Newton's second law. The equations of motion are integrated by a leapfrog-Verlet algorithm with a time step of $\Delta t = 0.01\tau$, in which

$$\tau = \left(\frac{m_{\mathrm{Ar}} \sigma_{\mathrm{Ar-Ar}}^2}{\varepsilon_{\mathrm{Ar-Ar}}} \right)^{1/2}. \qquad (4)$$

To reduce the time-consuming part of the calculation of interparticle forces, we mainly take two measures: (a) a typical potential cutoff of $r_{\mathrm{cut}} = 2.5\sigma_{\mathrm{Ar-Ar}}$ is used; (b) the link-cell method is adopted [31, 32].

The gas and wall temperatures are both fixed at $T = 119.8\,\mathrm{K}$. The velocity rescaling technique is applied to wall atoms to maintain a constant temperature. The fluid system is kept at a constant temperature by a Langevin thermostat method in the z direction. The motion equation of the ith molecule is

$$m\ddot{z}_i = \sum_{j \neq i} \frac{\partial \phi_{LJ}}{\partial z_i} - m\Gamma \dot{z}_i + \eta_i \qquad (5)$$

in which Γ is a friction constant determining the rate of heat exchange between the simulation system and the heat reservoir and η_i is a Gaussian distributed random force [33]. A general computation in our simulations requires approximately 1,000,000 time steps to obtain a fully developed flow. We then run additional 2,000,000 steps for averaging the macroscopic characteristics.

2.2. *Analytical methodology*

For the planar Poiseuille flow of a Newtonian fluid under a constant external force, the macroscopic hydrodynamics gives a simple parabolic solution of the Navier–Stokes equation with the consideration of the slip boundary condition

$$u_x = \frac{\rho g_x}{2\mu} (h^2 - z^2) + u_s \qquad (6)$$

in which z is the distance from the centreline of the microchannel, ρ is the density of the gas, μ is the shear viscosity, h is half of the width of the channel and u_s is the slip velocity [28]. The Navier boundary condition defines the slip velocity as

$$u_s = L_s \frac{\partial u}{\partial z} \bigg|_{\mathrm{wall}} \qquad (7)$$

in which L_s is the slip length. The dimensionless slip length is defined as $l_s = L_s/H$. Thus, the velocity profile of the Poiseuille flow can be rewritten as

$$u_x = \frac{\rho g_x}{2\mu} (h^2 + 2hl_s - z^2). \qquad (8)$$

Based on equation (8), we can extract the slip length by fitting the velocity profile obtained by our simulations.

For the slip boundary condition of a rarefied gas flowing over a solid, Maxwell theory predicts that the slip length is related to the molecular mean free path by

$$L_s = \alpha\lambda \qquad (9)$$

where $\alpha = (2 - f)/f$ is often called the slip constant. The mean free path of gas molecules in two-dimensional molecular dynamics can be calculated by

$$\lambda = \frac{1}{2\sqrt{2}n\sigma} \qquad (10)$$

in which n is the number density and σ is the diameter of gas molecules. The TMAC ranges from zero to unity under different solid surface conditions, such as gas species, solid material type, temperature, surface roughness and so on [35]. Thus, the slip constant for a given gas-solid condition should be larger than unity. Normalized by the system length, equation (9) can be written in dimensionless form:

$$l_s = \alpha Kn \qquad (11)$$

The Maxwell model shows two important characteristics: (1) the (dimensionless) slip length is linearly related to the mean free path (Knudsen number); (2) the slip constant, which is expected to be a constant independent of the Knudsen number, is from 1.0 to infinity. In the following sections, we will show pronounced deviations of the slip length of microscale gas flows from the Maxwell model induced by the surface roughness, which is here referred to as non-Maxwell slippage.

3. Results and discussion

3.1. *Maxwell slippage*

We first ascertain that rarefied gas flows in smooth microchannels and microchannels with very small surface roughness follow the Maxwell slippage at the boundaries by molecular dynamics simulations. Such simulations are also able to examine the validity of our calculations. The velocity profiles across the smooth microchannels and the boundary slips are shown in figure 2(a) and (b), respectively. The velocity profiles can present us the most fundamental information for understanding the microflow characteristics. However, it is almost not feasible for existing visualization techniques to experimentally observe the velocity profiles of microscale gas flows. In order to observe the velocity profile across the microchannels in our simulations, we divide the whole channel into many narrow bins to run averages of their macroscopic velocity. Figure 2(a) reports four of our seven runs of the velocity profiles. The velocities have been rescaled with a reference velocity $U = \sigma/\tau = 156\,\text{m/s}$. The shapes of the profile curves for different Knudsen numbers are not completely similar because the effective viscosity is a function of the Knudsen number for rarefied gases [36]. For gas flows in the slip regime, the macroscopic velocities at the walls in the x direction are apparently nonzero, in other words, there are velocity slips. As the Knudsen number increases, more pronounced slips can be observed at the walls. The rarefaction effect appears in the region adjacent to the walls, whose thickness is of the order of the molecular mean free path. Outside this region, all the velocity profiles are quadratic in the middle of the microchannels, which actually agrees with the prediction of equation (8). It indicates that the mainstream regime of the gas slip flows in the microchannels obeys the continuum mechanics characterized by the Navier–Stokes equations. Similar observations were also reported by other researchers [37, 38]. On the basis of the velocity profiles, the slip length can be calculated according to equation (8) as shown
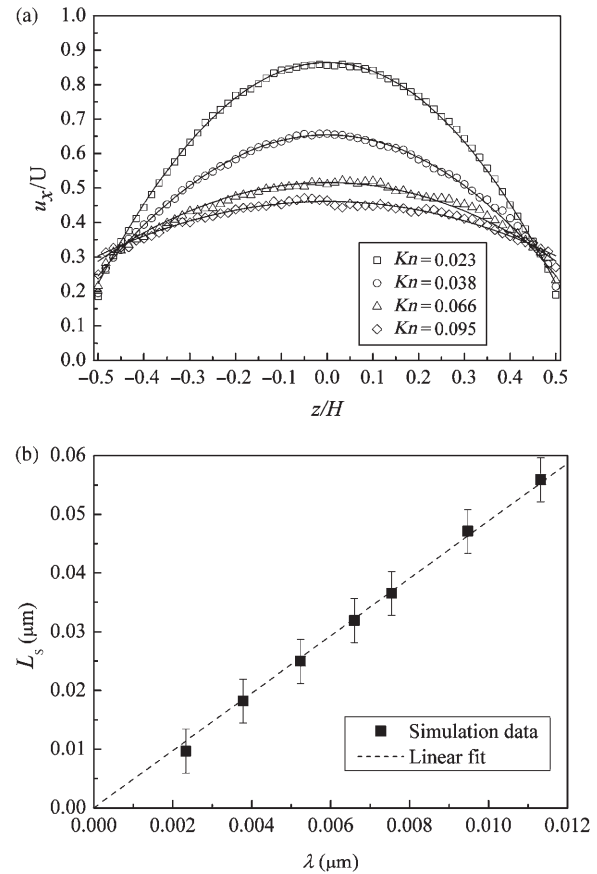
Figure 2. Characteristics of gas flows in smooth microchannels ($A = 0$). (a) Velocity profiles for various Knudsen numbers; (b) variation of slip length along with mean free path.

in figure 2(b). Clearly, the slip length is proportional to the mean free path where no-slip takes place as the Knudsen number goes to zero, which is in good agreement with the theoretical predictions by the Maxwell model. It also implies that the dimensionless slip length should be proportional to the Knudsen number. Fitted by a least-square method, the line gives the slip constant of $\alpha = 4.9$ for gaseous argon flowing over the smooth platinum surface, which agrees with the previous simulation data from Couette flows in [24, 35].

For gas flows in the microchannel with a surface roughness of $A = 1.2\,\text{nm}$, the flow profiles at various Knudsen numbers and the slip length depending on the mean free path are shown in figure 3(a) and (b). Though the channel surface is roughened, similar slip characteristics as the gas flows in smooth microchannels are observed, which indicates that the Maxwell model is applicable for small surface roughness. However, the slip constant is about 1.0 here, which tells us that this experiential value may be adopted in most microengineering situations [39, 40].
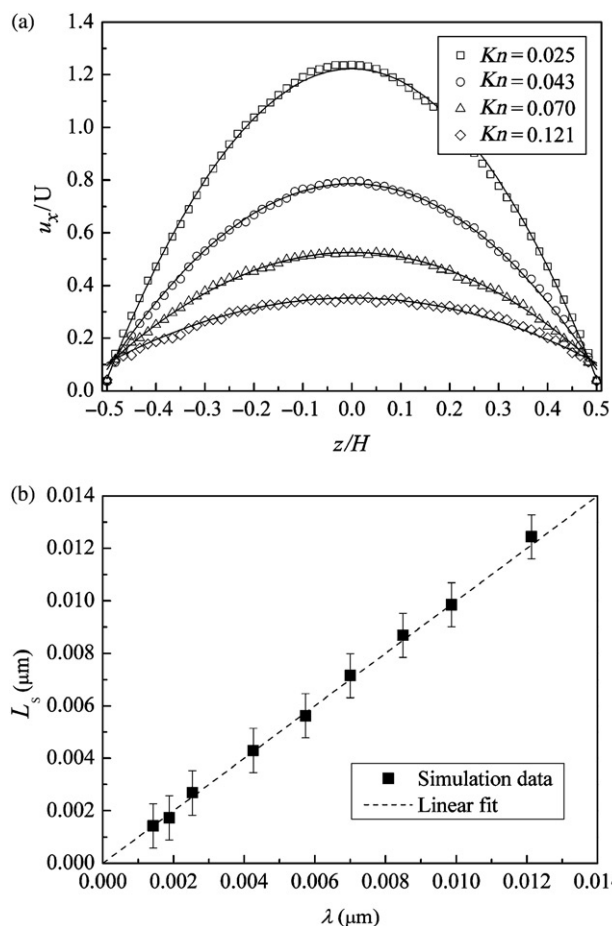
Figure 3. Characteristics of gas flows in microchannels with a surface roughness of $A = 1.2$ nm. (a) Velocity profiles for various Knudsen numbers; (b) variation of slip length along with mean free path.

Figure 4. Characteristics of gas flows in microchannels with a surface roughness of $A = 2.9$ nm. (a) Velocity profiles for various Knudsen numbers; (b) dependence of slip length on mean free path.

3.2. Non-Maxwell slippage

We now turn our attention to the non-Maxwell slippage at gas–solid interfaces induced by larger surface roughness. The velocity profiles and slip length of gas flows in microchannels with a surface roughness of $A = 2.9$ nm are taken as the first case as shown in figure 4(a) and (b). Figure 4(a) presents four of our ten runs of the velocity profiles obtained by our molecular dynamics simulations. The flows should fall into the slip regime according to the Knudsen numbers. Phenomenally, the slip velocities at walls become more pronounced with increasing Knudsen number. We also find that the slip velocities here are smaller than those in figure 3(a) for given Knudsen numbers (e.g. $Kn = 0.07$). For a smaller Knudsen number, e.g. $Kn = 0.03$, the velocity slip at the walls due to the rarefaction effect nearly disappears, which indicates that a non-slip boundary condition has been induced by the surface roughness.

The quantitatively analytical results are shown in figure 4(b). For convenience and guiding eyes, the variation of L_s/λ along with the mean free path is plotted. Figure 4(b) shows up two main characteristics: (1) L_s/λ is smaller than unity with Knudsen numbers ranging from 0.01 to 0.12 and even becomes negative with Knudsen number less than 0.03; (2) L_s/λ is a function of the mean free path, which indicates a nonlinear relation between the slip length and the Knudsen number. The nonlinear behaviour of the slip length is actually due to the comparability between the mean free path and the surface roughness (discussed in detail in the following section). These two characteristics both imply a significant deviation from the Maxwell model. The non-Maxwell slippage shows that the surface roughness may decrease the slip length. For smaller Knudsen numbers, the decrease is more pronounced. The slip length may be even decreased to negative.

Figure 5(a) and (b) show the velocity profiles and their slip characteristics of gas flows in microchannels
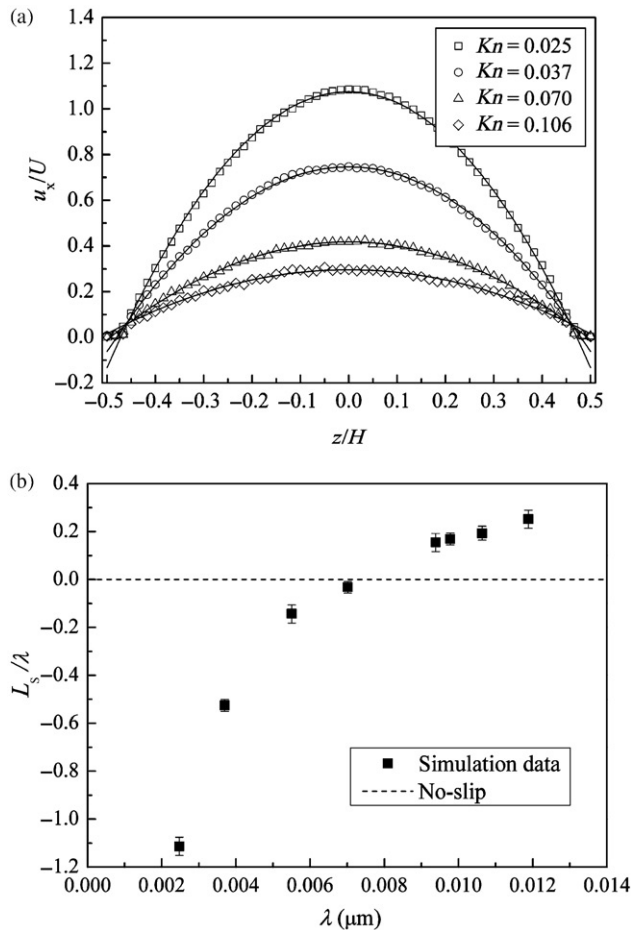
Figure 5. Characteristics of gas flows in microchannels with a surface roughness of $A = 6.0$ nm. (a) Velocity profiles for various Knudsen numbers; (b) dependence of slip length on mean free path.

with a surface roughness of $A = 6.0$ nm. In figure 5(a), the velocity profiles adjacent to the walls are clearly found to be distorted by the surface roughness. The averaged macroscopic velocities at the walls are about zero, which means that the gases beneath the surface roughness interspace are patches of backwater. The velocity slip can still be observed over the roughness element. When compared with the velocity profiles in figure 4(a), the larger surface roughness results in an additional deduction in the velocity slip. The velocity gradient becomes small in the wall-near regions. For rarefied gas flows with small Knudsen numbers (e.g. $Kn = 0.025$), the slip velocity is negative according to extrapolation of the Navier–Stokes equations based profile in the middle of the microchannels. Thus, the boundary slip is defined as a negative one, which was also adopted in describing the boundary conditions of nanoscale and macroscale flows [41–43]. As a result, the slip length is decreased to negative as the Knudsen
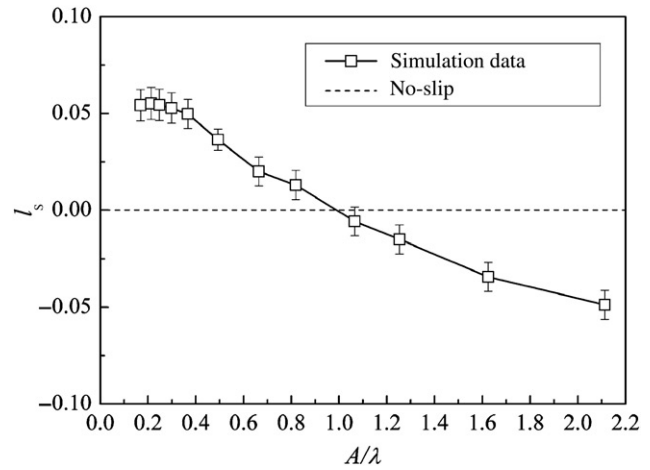
Figure 6. Slip length dependence on the ratio of mean free path to surface roughness size ($Kn = 0.055$).

number goes to zero as shown in figure 5(b). Though the Knudsen numbers are high enough to bring on apparent boundary slips according to the Maxwell theory and rarefied gas dynamics, the boundary conditions may show quite different characteristics because of the effect of the surface roughness. Hence, the Knudsen number alone is not rigorous enough to judge the slip behaviour at a wall.

3.3. Boundary conditions

The boundary conditions of gas flows in rough microchannels are found to depend not only on the Knudsen number but also on the surface roughness. General boundary conditions should consist of slip, no-slip and negative slip as demonstrated above. For $Kn = 0.055$, the effect of the surface roughness on the dimensionless slip length is shown in figure 6. The surface roughness is normalized by the ratio of the roughness size to the mean free path as suggested by Mo et al. [19]. Three types of boundary conditions, i.e. slip, no-slip and negative slip, are observed for rarefied gas flows in rough microchannels. For $A/\lambda \approx 1$, the slip length is nearly zero. It indicates that the no-slip boundary condition arises when the molecular mean free path is comparable with the surface roughness, which is in good agreement with Mo et al.'s results [19]. For $A/\lambda < 1$, the slip boundary condition due to rarefaction effect takes places. We also find that the slip length is independent of the roughness size when A/λ is smaller than 0.3. This supports the validity of the Maxwell model, which indicates that slip length is determined by the mean free path. For $A/\lambda > 1$, the slip becomes negative. This indicates that non-Maxwell slippage is a result of surface roughness being large
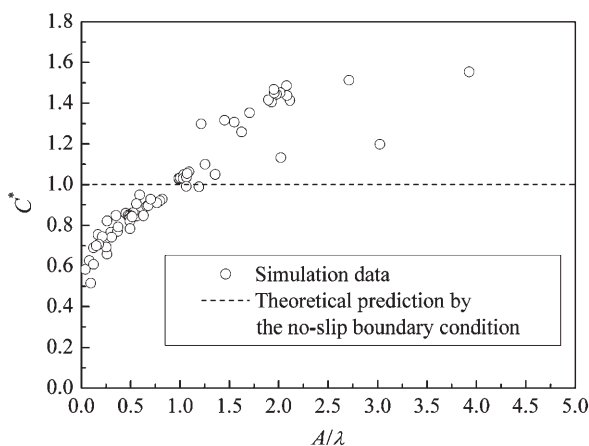
Figure 7. Friction dependence on the ratio of mean free path to surface roughness size for microscale gas flows.

with reference to the molecular mean free path, e.g. $A/\lambda \approx 0.3$.

We can also ascertain the boundary conditions of gas microflows according to their friction characteristics. For the locally fully developed laminar flows, the skin friction coefficient is defined as

$$f = \frac{\tau_w}{1/2(\rho u_0^2)} \tag{12}$$

in which τ_w is the wall shear stress calculated by the net change of momentum of gas molecules at a wall per unit area and time in our simulations, ρ is the density of gases and u_0 is the cross-sectionally averaged velocity. The product of the friction coefficient, f, and the Reynolds number, Re, is often referred to as the friction constant, i.e. $C = f\,\mathrm{Re}$. For a two-dimensional macroscopic flow, solving the Navier–Stokes equations theoretically with the no-slip boundary condition gives the friction constant $C_0 = 48$. If the Maxwell slip law is considered, the normalized friction constant C^*, which represents the deviation from flows on the macroscale, can be expressed as

$$C^* = \frac{C}{C_0} = \frac{1}{1 + 6l_s}. \tag{13}$$

This indicates that the rarefaction effect always reduces the friction of slip flows. Figure 7 shows the friction constants depending on the surface roughness. The friction coefficient for gas flows in microchannels may be lower, equal, or higher than that of flows on macroscale, which corresponds to the slip, no-slip, and negative slip boundary conditions according to equation (13). For $A/\lambda \approx 1$, the friction constant is

nearly equal to the theoretical results deduced from the Navier–Stokes equations with the no-slip boundary condition. It also indicates that the no-slip boundary condition arises when the molecular mean free path is comparable with the surface roughness. For $A/\lambda < 1$, the rarefaction effect, i.e. the boundary slip, decreases the friction. For $A/\lambda > 1$, however, the negative slip increases the friction. This shows that the non-Maxwell slippage induced by the surface roughness often increases the friction coefficient. The dispersion of our simulation data implies that the effects of the surface roughness and the rarefaction on the boundary conditions and friction coefficient are strongly coupled. Therefore, the criterion $A/\lambda \approx 1$ may be a good rule to validate the no-slip boundary condition for gases flowing over rough surfaces.

We have to ponder upon the reason why the surface roughness induces various boundary conditions. On the basis of the kinetic theory of gases, the interaction of gas molecules and a wall in the Maxwell theory is primarily based on the assumption of a bounce-back behaviour, which is a linear combination of diffusive and specular reflections. This assumption may be valid for mathematically smooth walls as demonstrated by the above simulation results. However, when the surface roughness is comparable with the molecular mean free path, this assumption is no longer rigorous. From our molecular simulations, the backwater gases beneath the roughness interspace may play an important role in the momentum exchange between gases and solid surfaces, because the molecules impinging the backwater may undergo multi-collisions inside the roughness interspace. Thus, the Knudsen layer and the wall roughness overlap. This means that the molecules can penetrate through the wall boundary region, which is different from an imaginary mathematical surface. The molecular behaviour combining multi-collisions and permeability are quite different from that adopted by theoretical analyses. Consequently, various boundary conditions are caused by the surface roughness.

4. Conclusions

We have investigated the boundary conditions of rarefied gas flows in rough microchannels by non-equilibrium molecular dynamics simulations. The Knudsen number is in the range 0.02–0.14 and the surface roughness is modelled by an array of triangular modules. The Maxwell model on slip length is found to break down due to the surface roughness for microscale gas flows in microchannels with large surface roughness. The non-Maxwell slippage shows that the slip length is smaller than the prediction of the Maxwell model and

is nonlinearly related to the molecular mean free path. For larger surface roughness and smaller Knudsen numbers, the non-Maxwell effect becomes more pronounced.

Induced by the surface roughness, the boundary conditions of microscale gas flows over rough surfaces should generally include slip, no-slip and negative slip. Our molecular dynamics simulations confirm that the criterion $A/\lambda \approx 1$ is a good rule to validate the no-slip boundary condition. For $A/\lambda < 1$, the slip boundary condition due to rarefaction effect takes places. For $A/\lambda > 1$, the slip becomes negative. Experientially, the Maxwell model is approximately applicable for $A/\lambda < 0.3$, but for A/λ greater than 0.3, non-Maxwell slippage arises. The boundary conditions depend on the coupling effects of the rarefaction and the surface roughness.

The permeability enhancement of a rough surface is demonstrated to be responsible for the roughness-induced non-Maxwell slippage. The backwater gases beneath the roughness interspace play an important role in the momentum exchange between gases and surfaces, because the molecules impinging the backwater may undergo multi-collisions in the roughness interspace. The molecular behaviour combining the penetrating and multi-collisions near a rough surface lead to the break-down of the bounce-back assumption used by the Maxwell theory.

References

[1] C. M. Ho and Y. C. Tai, Annu. Rev. Fluid Mech. **30,** 579 (1998).
[2] H. G. Craighead, Science **290,** 1532 (2001).
[3] P. Gravesen, J. Branebjerg, and O. S. Jensen, J. Micromech. Microeng. **3,** 168 (1993).
[4] N. Giordano and J. T. Cheng, J. Phys.: Condens. Matter **13,** R271 (2001).
[5] Z. Y. Guo and Z. X. Li, Int. J. Heat Mass Transfer **46,** 149 (2003).
[6] M. Gad-el-Hak, Mec. Ind. **2,** 313 (2001).
[7] M. Gad-el-Hak, Phys. Fluids **17,** 100612 (2005).
[8] T. M. Squires and S. R. Quake, Rev. Mod. Phys. **77,** 977 (2005).
[9] E. Lauga, M. P. Brenner, and H. A. Stone, *Handbook of Experimental Fluid Dynamics* (Springer, New York, 2005).
[10] S. A. Schaaf and P. L. Chambre, *Flow of Rarefied Gases* (Princeton University Press, New Jersey, 1961).
[11] A. A. Rostami, A. S. Majumdar, and N. Saniel, Heat Mass Transfer **38,** 339 (2002).
[12] G. E. Karniadakis and A. Beskok, *Micro Flows: Fundamentals and Simulation* (Springer-Verlag, New York, 2002).
[13] J. C. Maxwell, Phil. Trans. Roy. Soc. Part 1 **170,** 231 (1879).
[14] S. W. Kang, J. S. Chen, and J. Y. Hung, Int. J. Mach. Tools Manufact. **38,** 663 (1998).
[15] Z. Moktadir and K. Sato, Surf. Sci. **470,** L57 (2000).
[16] S. Richardson, J. Fluid Mech. **59,** 707 (1973).
[17] I. V. Volcov, Comput. Math. Math. Phys. **28,** 52 (1988).
[18] H. W. Sun and M. Gaghri, Numer. Heat Transfer A-Appl. **43,** 1 (2003).
[19] G. Mo and F. Rosenberger, Phys. Rev. A **42,** 4688 (1990).
[20] W. Sugiyama, T. Sawada, and K. Nakamori, Vacuum **6–8,** 791 (1996).
[21] S. E. Turner, L. C. Lam, and M. Faghri, J. Heat Transfer **126,** 753 (2004).
[22] B. Y. Cao, M. Chen, and Z. Y. Guo, Chin. Phys. Lett. **21,** 1777 (2004).
[23] B. Y. Cao, M. Chen, and Z. Y. Guo, Int. J. Eng. Sci. **44,** 927 (2006).
[24] B. Y. Cao, M. Chen, and Z. Y. Guo, Chin. Sci. Bull. **49,** 1101 (2004).
[25] K. P. Travis and K. E. Gubbins, J. Chem. Phys. **112,** 1984 (2000).
[26] D. X. Du, Effect of Compressibility and Roughness on Flow and Heat Transfer Characteristics in Microtubes. PhD Thesis, Tsinghua University, Beijing, 2000 (in Chinese).
[27] J. R. Hook and H. E. Hall, *Solid State Physics* (Wiley, Chichester, 1991).
[28] P. Yi, D. Poulikakos, J. Walther, and G. Yadigaroglu, Int. J. Heat Mass Transfer **45,** 2087 (2002).
[29] B. Y. Cao, M. Chen, and Z. Y. Guo, Chem. J. Chin. Univ. **26,** 277 (2005).
[30] B. Y. Cao, M. Chen, and Z. Y. Guo, Phys. Rev. E **74,** 066311 (2006).
[31] M. P. Allen and D. J. Tildesley, *Computer Simulation of Liquids* (Oxford University Press, New York, 1987).
[32] D. C. Rapaport, *The Art of Molecular Dynamics Simulation* (Cambridge University Press, New York, 1995).
[33] G. S. Grest and K. Kremer, Phys. Rev. A **33,** 3628 (1986).
[34] V. P. Sokhan, D. Nicholson, and N. Quirke, J. Chem. Phys. **115,** 3878 (2001).
[35] B. Y. Cao, M. Chen, and Z. Y. Guo, Appl. Phys. Lett. **86,** 091905 (2006).
[36] D. L. Morris, L. Hannon, and A. L. Garcia, Phys. Rev. A **46,** 5279 (1992).
[37] D. K. Bhattacharya and G. C. Lie, Phys. Rev. Lett. **62,** 897 (1989).
[38] M. Cieplak, J. Koplik, and J. R. Bavanar, Physica A **287,** 153 (2000).
[39] J. C. Harley, Y. F. Huang, H. H. Bau, and J. N. Zemel, J. Fluid Mech. **284,** 257 (1995).
[40] E. B. Arkilic, K. S. Breuer, and M. A. Schmidt, J. Fluid Mech. **437,** 29 (2001).
[41] P. A. Thompson and M. O. Robbins, Phys. Rev. A **41,** 6830 (1990).
[42] I. V. Ponomarev and A. E. Meyerovich, Phys. Rev. E **67,** 026302 (2003).
[43] A. D. Stroock, S. Dertinger, G. Whitesides, and A. Ajdari, Anal. Chem. **74,** 5306 (2002).